New Ternary Zirconium Antimonides, ZrSi$_{0.7}$Sb$_{1.3}$, ZrGeSb, and ZrSn$_{0.4}$Sb$_{1.6}$: A Family Containing ZrSiS-Type and β-ZrSb$_2$-Type Compounds

Robert Lam and Arthur Mar[1]

Department of Chemistry, University of Alberta, Edmonton, Alberta T6G 2G2, Canada

The ternary antimonides ZrSi$_{0.7}$Sb$_{1.3}$ and ZrGeSb have been synthesized through reaction of the elements at 1000 and 950°C, respectively, and their structures have been determined by single-crystal X-ray diffraction methods. They crystallize in the tetragonal space group D_{4h}^7-$P4/nmm$ with $Z = 2$ and cell dimensions of $a = 3.8091(2)$ Å and $c = 8.630(1)$ Å (ZrSi$_{0.7}$Sb$_{1.3}$) and $a = 3.8451(7)$ Å and $c = 8.634(2)$ Å (ZrGeSb) at $T = -50°$C. They represent new members, having one of the lowest total valence electron counts, of the large class of compounds MAB (M = transition metal; A, B = main-group elements) that adopt the ZrSiS-type structure containing stacked square nets. The ternary antimonide ZrSn$_{0.4}$Sb$_{1.6}$ has also been synthesized at 1000°C but it does not adopt the ZrSiS-type structure. Instead, it crystallizes in the orthorhombic space group D_{2h}^{16}-$Pnma$ with $a = 7.3187(6)$ Å, $b = 3.9618(4)$ Å, $c = 9.7076(7)$ Å, and $Z = 4$ ($T = -50°$C), adopting a structure that is a disordered variant of the known binary compound β-ZrSb$_2$. Reasons for the adoption of these two structure types are discussed. © 1997 Academic Press

INTRODUCTION

The PbFCl structure type, along with its relatives ZrSiS, BiOCl, Cu$_2$Sb, and Fe$_2$As, is an ubiquitous one with more than 200 members possessing diverse properties ranging from insulating–semiconducting to metallic (1, 2). Historically, despite significant differences among the "synonymous" structure types, all labels have been used interchangeably. The differences lie mainly in the degree of anion–anion bonding in the structure. For example, PbFCl itself is a "normal valence" compound consisting essentially of discrete F$^-$ and Cl$^-$ anions and is thus nonmetallic, whereas ZrSiS is deficient in electrons for the anions to satisfy the simple 8-n rule, so that fractional covalent

anion–anion bonds or metallic properties must result (3). Traditionally, "PbFCl" has been the label of choice in referring to members possessing this or its closely related structures. For clarity, we prefer the more accurate description "ZrSiS type" for the compounds ZrSi$_{0.7}$Sb$_{1.3}$ and ZrGeSb described herein, owing to the presence of anion–anion bonding, and reserve the label "PbFCl type" for cases in which no such bonding occurs.

Collectively, the PbFCl- or ZrSiS-type compounds may be designated as MAB (M = transition metal; A, B = main-group elements). The tetragonal structure consists of square nets of each of M, A, and B, stacked in the sequence [–A–M–B–B–M–A–], with the A net being twice as dense as the M or B net. The layers are held together by M–A and M–B bonds to produce an overall structure that, in most cases, is three-dimensional. The M atoms are surrounded by nine A or B atoms in a monocapped square antiprismatic geometry. These units are arranged in an alternating head-to-head and tail-to-tail fashion along the c axis.

A useful way to systematize members of the MAB family is to compare their c/a ratios, which separate two-dimensional from three-dimensional structures (2), and their valence electron counts, which measure the degree of anion–anion bonding. In normal valence compounds such as PbFCl, there is no deficiency of electrons ($\Delta = 0$) with respect to the simple 8-n rule (4). In polyanionic compounds, the greatest deficiency observed has been $\Delta = 2$, as in ZrSiS (5, 6) or NbSiAs (7), so that Si–Si half-bonds have to be invoked. Table 1 shows selected members with the PbFCl or ZrSiS structure type classified according to these two indicators. We report here two new compounds, ZrSi$_{0.7}$Sb$_{1.3}$ and ZrGeSb, that have three-dimensional ZrSiS-type structures and that have the most pronounced deficiency Δ yet observed in this family. In an attempt to synthesize the tin analogue, we show that the compound ZrSn$_{0.4}$Sb$_{1.6}$ reverts to a disordered variant of the binary compound β-ZrSb$_2$ (11). Possible reasons for the adoption of these structure types are presented.

---

[1] To whom correspondence should be addressed.

TABLE 1
Representative Ternary Compounds That Adopt the ZrSiS-Type (or PbFCl-Type) Structure

MAB	c/a	M–4B (Å)	M–B (Å)	A–A (Å)	Δ^a	Reference
UOTe	1.871	3.20	3.42	2.83	0	4
$ZrAs_{1.15}Se_{0.575}$	2.17	2.81(1)	2.886(5)	2.647(4)	0.6	8
$LaTe_2$	2.025	3.293(7)	3.260(7)	3.187(4)	1	9
ZrSiSe	2.30	2.76	3.01	2.57	2	5
ZrSiTe	2.572^b	2.918(1)	3.957(1)	2.614(1)	2	5, 10
ZrGeTe	2.224	2.93(1)	3.26(4)	2.734(1)	2	6
ZrSnTe	2.148	3.038(1)	3.086(1)	2.868(1)	2	2
NbSiAs	2.263	2.681(1)	2.811(1)	2.468(1)	2	7
$ZrSi_{0.7}Sb_{1.3}$	2.266	2.9460(3)	3.1085(7)	2.6934(1)	2.7	this work
ZrGeSb	2.245	2.9595(9)	3.094(2)	2.7189(5)	3	this work

$^a \Delta$ is defined as the deficiency of electrons available to the anions A and B with respect to satisfying the 8-n rule (4). For normal valence compounds, $\Delta = 0$. For ZrGeSb, a polyanionic compound, $\Delta = ((8 - 4) + (8 - 5)) - 4 = 3$.

^{b} High values of c/a (~ 2.6) correspond to layered compounds (1, 2, 5, 6).

EXPERIMENTAL

Synthesis

Reagents were elemental powders obtained from Cerac, Alfa-Aesar, or Aldrich, with $> 99.9\%$ purity (except for Zr, which was 99.7% pure). Reactions were carried out on a 0.250-g scale in evacuated fused-silica tubes (8-cm length; 10-mm i.d.). Elemental compositions (EDX analysis) of selected crystals were determined with the use of a Hitachi F2700 scanning electron microscope ($ZrSi_{0.7}Sb_{1.3}$ and $ZrSn_{0.4}Sb_{1.6}$) or a JEOL JSM-6301FXV field-emission scanning electron microscope (ZrGeSb and $ZrSn_{0.4}Sb_{1.6}$). X-ray powder patterns were obtained on an Enraf-Nonius FR552 Guinier camera ($CuK\alpha_1$ radiation; Si standard).

$ZrSi_{0.7}Sb_{1.3}$ was first identified in a reaction of La, Zr, and Sb in an $8:13:30$ ratio (intended for the preparation of La_3ZrSb_5 (12)). The mixture was heated at 600°C for 2 days and 1000°C for 2 days, after which it was cooled to 600°C over 2 days and to 20°C over 12 h. Shiny square plates were found at the walls of the partially attacked silica tube. Anal. (mol%): Zr, 31(1); Si, 22(1); Sb, 46(1) (average of three analyses). $ZrSi_{0.7}Sb_{1.3}$ can also be prepared more rationally by reaction of the elements. It can be formed from diverse loading compositions, except those that are Si-rich, in which case $ZrSi_2$ (13, 14) prevails as the major phase. For example, heating Zr, Si, and Sb in a $2:1:2$ ratio at 1000°C for 2 days followed by cooling to 500°C over 5 days and to 20°C over 12 h results in a mixture of binary impurities ZrSi (14) and $ZrSi_2$ (13, 14) (minor) as well as shiny square plates of the ternary compound. Anal. (mol%) Zr, 31(1); Si, 25(2); Sb, 44(3) (average of three analyses).

ZrGeSb resulted from a reaction of Zr, Ge, and Sb in a $1:1:3$ ratio, heated at 570°C for 1 day and then 950°C for 4 days, cooled to 500°C over 4 days, and finally cooled to 20°C over 12 h. The product consisted of square block-

shaped crystals of ZrGeSb and microcrystalline powder, containing the ternary compound as the major phase and unreacted Ge. Anal. (mol%): Zr, 32(1); Ge, 30(2); Sb, 38(1) (average of four analyses). ZrGeSb can be obtained from reactions with diverse loading compositions except those that are Ge-rich, in which case $ZrGe_2$ (15) is the major phase.

$ZrSn_{0.4}Sb_{1.6}$ was originally obtained as a byproduct from a reaction of La, Zr, Cu, and Sb in a $1:1:1:4$ ratio to which a 10-fold excess of Sn was added. The mixture was heated at 600°C for 1 day and then 900°C for 2 days, cooled to 600°C over 1 day, and finally cooled to 20°C over 10 h. Dissolving the Sn with concentrated HCl afforded a gray powder and black block-shaped crystals of $ZrSn_{0.4}Sb_{1.6}$, which were used in the structure determination. Except for compositions where Zr is in excess, reaction of the elements in various ratios at 1000°C for 2 days also results in $ZrSn_{0.4}Sb_{1.6}$. The ratio $2:1:2$ produced the best yield of $ZrSn_{0.4}Sb_{1.6}$ ($\sim 50\%$) as well as unreacted Sn and an unidentified minor phase.

The cell parameters of selected samples were refined from the powder diffraction data with the use of the program POLSQ (16). The observed and calculated interplanar distances, as well as intensities determined using the program LAZY-PULVERIX (17), are listed in Table S1 (18).

Structure Determination

Two crystals of $ZrSi_{0.7}Sb_{1.3}$, one from the original synthesis and one from the rational synthesis, as well as one each of ZrGeSb and $ZrSn_{0.4}Sb_{1.6}$, were selected. As the two $ZrSi_{0.7}Sb_{1.3}$ crystals gave essentially identical results (the refined compositions were $ZrSi_{0.68(1)}Sb_{1.32(1)}$ and $ZrSi_{0.74(2)}Sb_{1.26(1)}$ with similar metrical details), we report only the more accurate determination. Preliminary cell parameters were determined from Weissenberg photographs, which revealed Laue symmetry 4/mmm and systematic extinctions ($0kl: k + l = 2n + 1$) consistent with the tetragonal space groups D_{4h}^7-P4/nmm and D_{4h}^3-P4/n for $ZrSi_{0.7}Sb_{1.3}$ and ZrGeSb and Laue symmetry mmm and systematic extinctions ($0kl: k + l = 2n + 1$; $hk0: h = 2n + 1$) consistent with the orthorhombic space groups D_{2h}^{16}-Pnma and C_{2v}^9-$Pn2_1a$ for $ZrSn_{0.4}Sb_{1.6}$. Final cell parameters were determined from a least-squares analysis of the setting angles of 24 reflections centered on an Enraf-Nonius CAD4 diffractometer in the range $10° \leq 2\theta(MoK\alpha) \leq 20°$ for $ZrSi_{0.7}Sb_{1.3}$, $20° \leq 2\theta(MoK\alpha) \leq 50°$ for ZrGeSb, and $20° \leq 2\theta(MoK\alpha) \leq 39°$ for $ZrSn_{0.4}Sb_{1.6}$. Intensity data were collected at $-50°C$ with the θ–2θ scan technique in the range $4° \leq 2\theta(MoK\alpha) \leq 70°$. All calculations were carried out with the use of the SHELXTL (Version 5.0) package (19, 20). Conventional atomic scattering factors and anomalous dispersion corrections were used (21). Intensity data were reduced and averaged, and face-indexed

Gaussian-type absorption corrections were applied in XPREP. Initial atomic positions were found by direct methods in XS, and least-squares refinements were performed in XL.

For $ZrSi_{0.7}Sb_{1.3}$, the centrosymmetric space group $P4/nmm$ was chosen based on the intensity statistics and on the similarity of the intensity pattern to that of ZrSiS. An initial refinement assuming the formula ZrSiSb resulted in reasonable displacement parameters for all sites except the one at $\frac{3}{4}$, $\frac{1}{4}$, 0, for which the displacement parameter was anomalously low. Since disordering of the nonmetal atoms in this site has previously been observed (2), a refinement was performed in which the two possible nonmetal sites were allowed to be fully occupied by a mixture of Si and Sb, with no constraint placed on the overall Si : Sb ratio. This resulted in occupancies of 98(1)% Sb and 2(2)% Si in the site $\frac{1}{4}$, $\frac{1}{4}$, 0.61 and 74(2)% Si and 26(1)% Sb in the site $\frac{3}{4}$, $\frac{1}{4}$, 0. The final refined formula, assuming the former site is fully occupied by Sb, is $ZrSi_{0.74(2)}Sb_{1.26(1)}$, which agrees well with the EDX analysis. Disorder appears to be an inherent property in this compound, and we shall accept the formulation $Zr(Si_{0.7}Sb_{0.3})Sb$ or $ZrSi_{0.7}Sb_{1.3}$.

For ZrGeSb, the space group $P4/nmm$ was chosen based on the similarity of the intensity pattern with that of $ZrSi_{0.7}Sb_{1.3}$, despite a high R_{int} index for averaging (which we attribute to the difficulty in performing a good absorption correction). Refinements in which the occupancies of successive atoms were allowed to vary (while the isotropic displacement parameters were fixed) resulted in values of 99.4(7)% for Zr, 102.5(6)% for Ge, and 98.7(6)% for Sb. A refinement performed allowing the nonmetal sites to be disordered resulted in occupancies of 90(4)% Ge in one site and 98(3)% Sb in the other site. Thus, in contrast to $ZrSi_{0.7}Sb_{1.3}$, we accept the ordered model for ZrGeSb.

$ZrSn_{0.4}Sb_{1.6}$ was recognized to be isotypic to β-$ZrSb_2$ (11). Because of their similar scattering factors, it is not possible to distinguish between Sn and Sb from the X-ray data alone. In other ternary compounds containing Sn and Sb (22), an ordered model can be invoked because of their very different coordination geometries. In this case, however, there is no compelling reason to do so because the environments of the two anion sites $X(1)$ and $X(2)$ are chemically indistinguishable: both sites together complete the monocapped square antiprismatic coordination around the Zr atom. Refinements in which these sites were occupied completely either by Sn or Sb produced identical results. Independent refinements of the site occupation factors of $X(1)$ and $X(2)$ (whether they were filled by Sn or Sb), as well as the Zr site, confirmed essentially 100% occupancy. Since the cell constants of $ZrSn_{0.4}Sb_{1.6}$ ($a = 7.3187(6)$ Å, $b = 3.9618(4)$ Å, $c = 9.7076(7)$ Å, $V = 281.47(4)$ Å^3; $T = -50°C$) deviate significantly from those of β-$ZrSb_2$ ($a = 7.393(1)$ Å, $b = 3.9870(7)$ Å, $c = 9.581(1)$ Å, $V = 282.42(7)$ Å^3; $T = 25°C$) (11) (more than can be accounted

for even by the difference in temperature), partial substitution of larger Sn atoms for Sb atoms must have occurred. Ultimate composition was established from EDX analyses on two scanning electron microscopes. Averaging eight analyses resulted in atomic percentages of 29(2)% Zr, 13(1)% Sn, and 58(2)% Sb (JEOL JSM-6301FXV), while averaging five resulted in 36(4)% Zr, 11(1)% Sn, and 53(3)% Sb (Hitachi F2700). The discrepancies arise from use of different calibration standards. These analyses are consistent with a formula "$ZrSn_{0.4}Sb_{1.6}$" (33% Zr, 13% Sn, 53% Sb). Sites $X(1)$ and $X(2)$ were thus occupied by a mixture of 20% Sn and 80% Sb in the final refinement.

The displacement parameters are unexceptional, and difference electron density maps are featureless ($ZrSi_{0.7}Sb_{1.3}$: $\Delta\rho_{max} = 1.00$, $\Delta\rho_{min} = -1.72$; ZrGeSb: $\Delta\rho_{max} = 5.81$, $\Delta\rho_{min} = -11.30$; $ZrSn_{0.4}Sb_{1.6}$: $\Delta\rho_{max} = 4.44$; $\Delta\rho_{min} = -4.95\ e^-\ Å^{-3}$). Crystal data and further details of the data collection are given in Tables 2 and S2 (18). Final values of the positional and displacement parameters are given in Table 3. Selected interatomic distances are given in Table 4. Anisotropic displacement parameters are given in Table S3, interatomic angles in Tables S4 and S5, and final structure amplitudes are in Tables S6–S8 (18).

RESULTS AND DISCUSSION

Synthesis

The use of silica tubes in high-temperature solid-state reactions sometimes leads to materials incorporating Si or SiO_2 (2, 6, 23), as was the case in the original synthesis of $ZrSi_{0.7}Sb_{1.3}$. This compound can also be formed by direct reaction of the elements at most compositions except those that are Si-rich, in which case formation of the binary $ZrSi_2$ predominates. The preferred formation of $ZrSi_2$ in ternary phase reactions has been documented (5). Similarly, in the ZrGeSb system, the thermodynamically more stable phase, $ZrGe_2$, was the major product in all Ge-rich reactions. Related observations have been noted in the syntheses of ternary zirconium silicon/germanium chalcogenides, whose thermal stability decreases with increasing formula weight (5). Since the most convenient temperatures for crystal growth of the ternary compounds are also precariously close to their decomposition region, it is difficult to obtain them in pure form. The nonexistence of a "ZrSnSb" phase with the ZrSiS-type structure may be attributed to this trend in decreasing thermal stability, but other, structural reasons may be important.

The cell parameters refined from X-ray powder patterns resulting from compositionally diverse preparations of $ZrSi_{0.7}Sb_{1.3}$, ZrGeSb, and $ZrSn_{0.4}Sb_{1.6}$ do not vary significantly. In particular, the cell volume remains relatively constant in different preparations of $ZrSi_{0.7}Sb_{1.3}$. Moreover, in the case of $ZrSi_{0.7}Sb_{1.3}$, the two crystals examined were obtained under very different synthetic conditions, but

TABLE 2
Crystallographic Data for $ZrSi_{0.7}Sb_{1.3}$, ZrGeSb, and $ZrSn_{0.4}Sb_{1.6}$

	$ZrSi_{0.74(2)}Sb_{1.26(1)}$	ZrGeSb	$ZrSn_{0.4}Sb_{1.6}$
Formula	$ZrSi_{0.74(2)}Sb_{1.26(1)}$	ZrGeSb	$ZrSn_{0.4}Sb_{1.6}$
Formula mass (amu)	264.80	285.56	330.50
Space group	$P4/nmm$ (No. 129)	$P4/nmm$ (No. 129)	$Pnma$ (No. 62)
a (Å)	3.8091(2)[a]	3.8451(7)[a]	7.3187(6)[b]
b (Å)	—	—	3.9618(4)[b]
c (Å)	8.630(1)[a]	8.634(2)[a]	9.7076(7)[b]
V (Å³)	125.22(2)	127.66(4)	281.47(4)
Z	2	2	4
T (°C)	−50	−50	−50
ρ_{calc} (g cm⁻³)	7.023	7.429	7.870
Radiation	$MoK\alpha, \lambda = 0.71073$ Å	$MoK\alpha, \lambda = 0.71073$ Å	$MoK\alpha, \lambda = 0.71073$ Å
$\mu(MoK\alpha)$ (cm⁻¹)	175.8	258.0	220.4
No. of data collected	2138	2158	2484
No. of unique data, including $F_o^2 < 0$	203 ($R_{int} = 0.068$)	203 ($R_{int} = 0.269$)	690 ($R_{int} = 0.127$)
No. of unique data, with $F_o^2 > 2\sigma(F_o^2)$	202	197	663
No. of variables	12	10	20
$R(F)$ for $F_o^2 > 2\sigma(F_o^2)$[c]	0.015	0.062	0.048
$R_w(F_o^2)$[d]	0.039	0.144	0.107

[a] Obtained from a refinement constrained so that $a = b$ and $\alpha = \beta = \gamma = 90°$.
[b] Obtained from a refinement constrained so that $\alpha = \beta = \gamma = 90°$.
[c] $R(F) = \sum ||F_o| - |F_c||/\sum |F_o|$.
[d] $R_w(F_o^2) = [\sum [w(F_o^2 - F_c^2)^2]/\sum wF_o^4]^{1/2}$; $w^{-1} = [\sigma^2(F_o^2) + (Ap)^2 + Bp]$, where $p = [\max(F_o^2, 0) + 2F_c^2]/3$, $A = 0.0029, 0.0601$, and 0.0600, and $B = 0.34, 2.36$, and 1.71 for $ZrSi_{0.7}Sb_{1.3}$, ZrGeSb, and $ZrSn_{0.4}Sb_{1.6}$, respectively.

their compositions refined from the X-ray data are essentially identical. The degree of nonhomogeneity in these compounds is probably slight, if any.

Structure of $ZrSi_{0.7}Sb_{1.3}$ and ZrGeSb

These adopt the ZrSiS-type structure, which has been described in detail previously (1–7). Briefly, the Zr atoms reside in a monocapped square antiprismatic environment (CN 9). Four A atoms form the basal square plane ($A =$ Si and Sb(1) in $ZrSi_{0.7}Sb_{1.3}$ or Ge atoms in ZrGeSb), four Sb(2) atoms form a larger square twisted 45° relative to the first one, and a fifth Sb(2) atom caps this square. If the capping Sb atom is designated as the "head," then the structure can be described as an arrangement of monocapped square antiprisms oriented head-to-head and tail-to-tail (Fig. 1a).

TABLE 3
Positional and Equivalent Isotropic Thermal Parameters for $ZrSi_{0.7}Sb_{1.3}$, ZrGeSb, and $ZrSn_{0.4}Sb_{1.6}$

| Atom	Wyckoff position	x	y	z	U_{eq} (Å²)[a]
		$ZrSi_{0.74(2)}Sb_{1.26(1)}$			
Zr	$2c$	$\frac{1}{4}$	$\frac{1}{4}$	0.25076(6)	0.0054(2)
A[b]	$2a$	$\frac{3}{4}$	$\frac{1}{4}$	0	0.0080(3)
Sb(2)	$2c$	$\frac{1}{4}$	$\frac{1}{4}$	0.61095(4)	0.0056(2)
		ZrGeSb			
Zr	$2c$	$\frac{1}{4}$	$\frac{1}{4}$	0.2532(2)	0.0049(6)
Ge	$2a$	$\frac{3}{4}$	$\frac{1}{4}$	0	0.0052(5)
Sb	$2c$	$\frac{1}{4}$	$\frac{1}{4}$	0.6115(1)	0.0051(5)
		$ZrSn_{0.4}Sb_{1.6}$			
Zr	$4c$	0.26110(9)	$\frac{1}{4}$	0.16278(6)	0.0047(2)
$X(1)$[c]	$4c$	0.86981(6)	$\frac{1}{4}$	0.04578(4)	0.0057(2)
$X(2)$[c]	$4c$	0.92828(6)	$\frac{1}{4}$	0.64836(4)	0.0053(2)

[a] U_{eq} is defined as one-third of the trace of the orthogonalized U_{ij} tensor.
[b] A contains 74(2)% Si and 26(1)% Sb(1).
[c] Each site is occupied by 20% Sn and 80% Sb.

TABLE 4
Selected Interatomic Distances (Å) in $ZrSi_{0.7}Sb_{1.3}$, ZrGeSb, and $ZrSn_{0.4}Sb_{1.6}$

	$ZrSi_{0.74(2)}Sb_{1.26(1)}$	ZrGeSb
Zr–Sb(2) (×4)	2.9460(3)	2.9595(9)
Zr–Sb(2)	3.1085(7)	3.094(2)
Zr–A (×4)	2.8829(4)	2.911(1)
A–A (×4)	2.6934(1)	2.7189(5)
Sb(2)–Sb(2) (×4)	3.3049(4)	3.331(1)
	$ZrSn_{0.4}Sb_{1.6}$	
Zr–$X(1)$	2.9389(8)	
Zr–$X(1)$ (×2)	2.9902(6)	
Zr–$X(2)$ (×2)	3.0186(6)	
Zr–$X(2)$ (×2)	3.0342(6)	
Zr–$X(1)$	3.0808(9)	
Zr–$X(2)$	3.2588(8)	
$X(1)$–$X(1)$ (×2)	2.8888(7)	
$X(1)$–$X(2)$ (×2)	3.1105(5)	
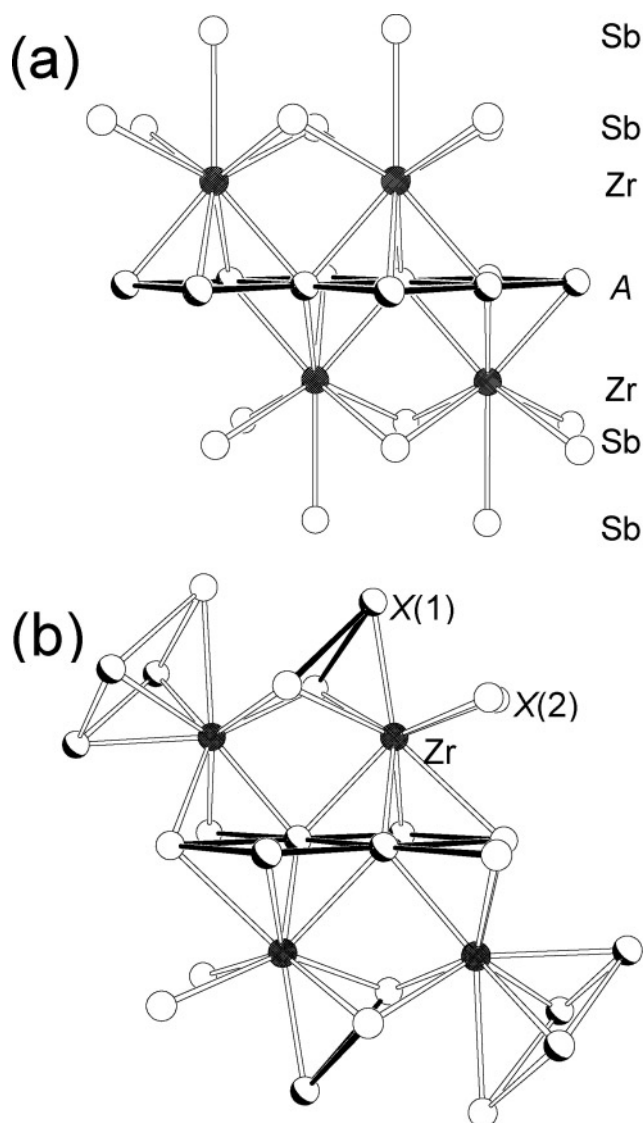
FIG. 1. Connectivity of monocapped square antiprismatic coordination polyhedra in (a) $ZrSi_{0.7}Sb_{1.3}$ and ZrGeSb and (b) $ZrSn_{0.4}Sb_{1.6}$. The darkened bonds represent planes of bonding atoms within the structures. Site A contains 74(2)% Si and 26(1)% Sb(1) in $ZrSi_{0.7}Sb_{1.3}$ and 100% Ge atoms in ZrGeSb. Sites $X(1)$ and $X(2)$ are occupied by 20% Sn and 80% Sb in $ZrSn_{0.4}Sb_{1.6}$. $ZrSi_{0.7}Sb_{1.3}$ and ZrGeSb adopt the ZrSiS-type structure, while $ZrSn_{0.4}Sb_{1.6}$ adopts the β-$ZrSb_2$-type structure. Note the tail-to-tail (and head-to-head) orientation of the building units in the Si and Ge compounds in contrast to the head-to-tail orientation in the Sn compound.

Examination of Table 4 shows that most bonds are lengthened on going from $ZrSi_{0.7}Sb_{1.3}$ to ZrGeSb, consistent with substitution of Si by the larger Ge atom, although the increase may not be as pronounced as expected. In fact, the bond from Zr to the capping Sb atom is shorter in ZrGeSb (3.094(2) Å) than in $ZrSi_{0.7}Sb_{1.3}$ (3.1085(7) Å). This results from relief of steric crowding of the Sb atoms within the Sb squares and the presence of longer Ge–Ge bonds,

thus allowing the capping Sb atom to better interact with the Zr center (2).

The Sb–Sb separations (>3.3 Å) within the less dense square net are too long to be bonding. Within the denser square net of A atoms, the A–A distances are 2.6934(1) Å for $ZrSi_{0.7}Sb_{1.3}$ and 2.7189(5) Å for ZrGeSb. These distances fall outside of the range normally considered for a full Si–Si or Ge–Ge single bond. For example, such bonds are found in many ternary main-group pnictides $A_xM_yPn_z$ (A = alkali metal or alkaline earth; M = tetrel; Pn = P, As, Sb, Bi), where Si–Si (24–28) and Ge–Ge (24, 25, 29, 30) single-bond distances are ~ 2.3–2.4 and ~ 2.4–2.5 Å, respectively. The corresponding distances in $ZrSi_{0.7}Sb_{1.3}$ and ZrGeSb are about 10–15% longer, suggesting that these bonds are of fractional order. The large number of MAB compounds may be organized along a continuum in which at one extreme lie PbFCl-type members that are nonmetallic or "normal valence" compounds (4, 31, 32). For example, the formulation for UOTe may be represented as $U^{4+}(O^{2-})$ (Te^{2-}). More importantly, the M cation provides sufficient electrons to the A and B atoms to satisfy the octet rule, so formation of anion–anion bonds in the square A net is excluded and the structure consists of discrete ions. Representatives of nonmetallic PbFCl-type compounds include the oxyhalides $PuOX$ (X = Cl, Br, I) (4) and oxychalcogenides UOY (Y = S, Se, Te) (4). At the other extreme are found the more metallic phases in which the M cation provides insufficient electrons to saturate the valence requirements of A and B. These ZrSiS-type compounds necessarily contain A–A bonds of fractional order which have now been quantified by band structure calculations (1). The degree of anion–anion interaction within the square nets of A atoms depends on the size of the cation as well as the anion (4). Examples of these metallic phases are provided by the ternary main-group chalcogenides given in Table 1.

The dimensionality of ZrSiS-type structures has also been studied previously (2). The transition from a three-dimensional to a true layered structure depends on the distance from M to the capping B atom and is signaled by an anomalously high c/a ratio. In the series $ZrAB$ (A = Si, Ge, Sn; B = S, Se, Te), ZrSiTe is shown to be a layered compound as indicated by its high c/a ratio (2.572) compared to normal values of 2.0–2.3 for three-dimensional structures (Table 1) (1, 2, 5, 6). This ratio also provides a useful division between metallic and nonmetallic phases, as values for the former do not fall below 2.0 (4).

We can now classify $ZrSi_{0.7}Sb_{1.3}$ and ZrGeSb according to electron count, ionic–metallic distinction, and dimensionality. As shown in Table 1, most ZrSiS-type compounds have electron counts that correspond to a deficiency Δ of two electrons required for the A and B atoms to satisfy the 8-n rule. Consequently, the A–A bonds within the denser square net are often portrayed as half-bonds, or one-electron bonds. $ZrSi_{0.7}Sb_{1.3}$ and ZrGeSb are noteworthy in

having the largest value of $\Delta = 3$ while retaining the ZrSiS-type structure. Interestingly, the Ge–Ge distance in ZrGeSb (2.7189(5) Å) is not significantly different from that in ZrGeTe (2.734(1) Å) (6). Presumably, other factors, such as the complex interplay of Zr–A and Zr–B bonds as well as steric effects, are important in controlling the stability of this structure type. A thorough band structure study is needed to unravel these complexities. In terms of bonding character, $ZrSi_{0.7}Sb_{1.3}$ and ZrGeSb belong to the more metallic phases containing fractional anion–anion bonds. Examination of the Zr–Sb(capping) distances in $ZrSi_{0.7}Sb_{1.3}$ (3.1085(7) Å) and ZrGeSb (3.094(2) Å) indicates that these are three-dimensional structures, as confirmed by their c/a ratios (2.266 and 2.245, respectively).

A reasonable explanation for nonstoichiometry in $ZrSi_{0.7}Sb_{1.3}$ and its absence in ZrGeSb may be attributed to the size difference between Si and Ge. Note that the anion–anion (A–A) distance remains fairly constant as one substitutes Si with Ge (~ 2.7 Å). This suggests that bond distances within the square net of smaller A atoms are already *fixed* by the constraint imposed by the presence of the larger Sb atoms in the less dense square B net. Placing only Si atoms in the geometrically fixed sites in the square A net would result in an unstable compound because the A–A distances are too far for even fractional Si–Si bonding to be strong enough to provide sufficient bonding energy. Thus, $ZrSi_{0.7}Sb_{1.3}$ requires replacement of approximately every fourth Si atom with the larger Sb atom in the square net to achieve sufficient anion–anion bonding to stabilize the compound. Furthermore, we would not expect much variability in the nonstoichiometric formula for $ZrSi_{0.7}Sb_{1.3}$ since the degree of disorder is defined by the structurally constrained anion–anion distances. In contrast, for ZrGeSb, the insertion of the larger Ge atoms into site $2a$ results in sufficient anion–anion bonding to satisfy the electronic demands of the structure, thus giving rise to the stoichiometric and ordered formula ZrGeSb. Examples exist in which the size of the anionic square net does not remain constant in related series of compounds. For instance, the compounds ZrATe ($A =$ Si, Ge, Sn) (2, 5, 6) show that as the size of the A atoms in the square net increases, the A–A bond distance increases significantly from 2.61 to 2.87 Å (Table 1). However, other systems such as UAS ($A =$ Si, Ge) (31), UATe ($A =$ Sn, Sb) (31), ZrAS ($A =$ Si, Ge) (5), HfAS ($A =$ Si, Ge) (5), and HfASe ($A =$ Si, Ge) (5) do support the trend that the square nets of A atoms remain relatively unperturbed by the effects of substitution.

Structure of $ZrSn_{0.4}Sb_{1.6}$

We attempted to synthesize "ZrSnSb" to see if it would adopt the ZrSiS-type structure as well. Instead, we obtained the compound $ZrSn_{0.4}Sb_{1.6}$, a disordered variant of β-$ZrSb_2$ which is of the PbCl$_2$-type. The structure of β-$ZrSb_2$

has been described in detail before (11). In $ZrSn_{0.4}Sb_{1.6}$, the two anion sites $X(1)$ and $X(2)$ are disordered, containing a mixture of 20% Sn and 80% Sb. Bond distances and angles are generally similar to those of the parent compound, with some irregular variations. The structure of $ZrSn_{0.4}Sb_{1.6}$ is related to the ZrSiS-type structures of $ZrSi_{0.7}Sb_{1.3}$ and ZrGeSb in that they are based on Zr-centered monocapped square antiprisms. These units are undistorted in $ZrSi_{0.7}Sb_{1.3}$ and ZrGeSb but distorted in $ZrSn_{0.4}Sb_{1.6}$, with irregular squares and a tilted capping atom. The capping atom in such units can often be found with varying tilt angles (33). If the "capping" atom is again designated as the "head," then the structure of $ZrSn_{0.4}Sb_{1.6}$ can be built up from these units, aligned in a head-to-tail fashion and pointing in several directions (Fig. 1b). In contrast to the ZrSiS-type structure, the structure no longer consists of parallel square nets, but rather staggered "ribbons" that are four atoms wide.

Implications

The discontinuity of structure type upon substitution of Sn may be rationalized by the size differences of the Group 14 atoms. Haneveld and Jellinek provided a useful index for predicting the occurrence of the PbFCl structure type in MAB compounds, based on the ratio of the radii of the metal M and the elements A and B (31). As shown in Table 1, the M–4B distances are always larger than the A–A distances and in instances in which this is not true, the resulting compound either does not exist or adopts a different structure type. When the condition is met, the resulting compound adopts either the PbFCl/ZrSiS structure type (in most cases) or the closely related tetragonal ($I4/mmm$) UGeTe structure type (31). In the present case, if we accept that *most* regular Sn–Sn single-bond distances in the solid state lie in the range 2.804–2.891 Å (34–36), with a few examples of slightly longer distances such as 2.984 Å (37), then it is reasonable that $ZrSn_{0.4}Sb_{1.6}$ prefers not to crystallize in the space group $P4/nmm$ since the Zr–4Sb distances for a hypothetical ZrSiS-type compound "ZrSnSb" are expected to be at least 2.96 Å. Thus, $ZrSn_{0.4}Sb_{1.6}$ appears to be at the limit for the formation of the MAB structure type. The fact that similarities can be drawn between the two structure types (ZrSiS and β-$ZrSb_2$) is probably an indication that $ZrSn_{0.4}Sb_{1.6}$ lies at the border between the two types. It is interesting to note that if Sb is substituted by Te, which has a similar atomic radius, the MAB member ZrSnTe (2) exists with Zr–4Te and Sn–Sn distances of 3.038(1) and 2.867(1) Å, respectively. We believe Haneveld and Jellinek's model accounts for most observations but is not applicable in all cases.

The preparation of this series of compounds illustrates the great versatility of the PbFCl or ZrSiS structure type. The physical properties of these compounds, which are

expected to be metallic conductors (2, 4, 32, 38), are being investigated. A band structure calculation will help clarify the factors involved in their stability. It would be interesting to see if ZrSiS-type "TiSnSb" or "HfSnSb" compounds can be made, if "ZrSnSb" has not. The transition metal and main-group elements can also be substituted to probe the limits of this diverse structural class.

ACKNOWLEDGMENTS

REFERENCES

1. W. Tremel and R. Hoffmann, *J. Am. Chem. Soc.* **109,** 124 (1987).
2. C. Wang and T. Hughbanks, *Inorg. Chem.* **34,** 5524 (1995).
3. U. Müller, "Inorganic Structural Chemistry." Wiley, New York, 1993.
4. F. Hulliger, *J. Less-Common Met.* **16,** 113 (1968).
5. H. Onken, K. Vierheilig, and H. Hahn, *Z. Anorg. Allg. Chem.* **333,** 267 (1964).
6. A. J. K. Haneveld and F. Jellinek, *Recl. Trav. Chim. Pays-Bas* **83,** 776 (1964).
7. V. Johnson and W. Jeitschko, *J. Solid State Chem.* **6,** 306 (1973).
8. J. C. Barthelat and Y. Jeannin, *J. Less-Common Met.* **26,** 273 (1972).
9. R. Wang, H. Steinfink, and W. F. Bradley, *Inorg. Chem.* **5,** 142 (1966).
10. W. Bensch and P. Dürichen, *Acta Crystallogr., Sect. C: Cryst. Struct. Commun.* **50,** 346 (1994).
11. E. Garcia and J. D. Corbett, *J. Solid State Chem.* **73,** 452 (1988).
12. G. Bolloré, M. J. Ferguson, R. W. Hushagen, and A. Mar, *Chem. Mater.* **7,** 2229 (1995).
13. S. Náray-Szabó, *Z. Kristallogr.* **97,** 223 (1937).
14. H. Schachner, H. Nowotny, and H. Kudielka, *Monatsh. Chem.* **85,** 1140 (1954).
15. J. F. Smith and D. M. Bailey, *Acta Crystallogr.* **10,** 341 (1957).
16. "POLSQ: Program for Least-Squares Unit Cell Refinement," 1983 [modified by D. Cahen and D. Keszler, Northwestern University].
17. K. Yvon, W. Jeitschko, and E. Parthé, *J. Appl. Crystallogr.* **10,** 73 (1977).
18. See NAPS document No. 05437 for 18 pages of supplementary material. This is not a multi-article document. Order from NAPS c/o Microfiche Publications, P.O. Box 3513, Grand Central Station, New York, NY 10163-3513. Remit in advance in U.S. funds only $7.75 for photocopies or $5.00 for microfiche. There is a $15.00 invoicing charge on all orders filled before payment. Outside U.S. and Canada add postage of $4.50 for the first 20 pages and $1.00 for each 10 pages of material thereafter, $1.75 for the first microfiche and $.50 for each microfiche thereafter.
19. G. M. Sheldrick, "SHELXTL," Version 5.0, Siemens Analytical X-ray Instruments, Inc., Madison, WI, 1994.
20. G. M. Sheldrick, *J. Appl. Crystallogr.*, in press.
21. "International Tables for X-ray Crystallography" (Wilson, A. J. C., Ed.), Vol. C. Kluwer: Dordrecht, 1992.
22. R. Lam and A. Mar, *Inorg. Chem.* **35,** 6959 (1996).
23. F. Jellinek and H. Hahn, *Naturwissenschaften* **49,** 103 (1962).
24. B. Eisenmann and H. Schäfer, *Angew. Chem., Int. Ed. Engl.* **19,** 490 (1980).
25. B. Eisenmann and H. Schäfer, *Z. Anorg. Allg. Chem.* **484,** 142 (1982).
26. P. M. Hamon, J. Guyader, P. L'Haridon, and Y. Laurent, *Acta Crystallogr., Sect. B: Struct. Crystallogr. Cryst. Chem.* **31,** 445 (1975).
27. W.-M. Hurng, J. D. Corbett, S.-L. Wang, and R. A. Jacobson, *Inorg. Chem.* **26,** 2392 (1987).
28. B. Eisenmann, H. Jordan, and H. Schäfer, *Z. Naturforsch., B: Anorg. Chem., Org. Chem.* **39,** 864 (1984).
29. B. Eisenmann, H. Jordan, and H. Schäfer, *Z. Naturforsch., B: Anorg. Chem., Org. Chem.* **37,** 1221 (1982).
30. B. Eisenmann and H. Schäfer, *Z. Naturforsch., B: Anorg. Chem., Org. Chem.* **36,** 415 (1981).
31. A. J. K. Haneveld and F. Jellinek, *J. Less-Common Met.* **18,** 123 (1969).
32. F. Hulliger, *J. Less-Common Met.* **30,** 397 (1973).
33. M. J. Ferguson, R. W. Hushagen, and A. Mar, *Inorg. Chem.* **35,** 4505 (1996).
34. B. Eisenmann, H. Jordan, and H. Schäfer, *Z. Anorg. Allg. Chem.* **532,** 73 (1986).
35. B. Eisenmann, H. Jordan, and H. Schäfer, *Z. Naturforsch., B: Anorg. Chem., Org. Chem.* **38,** 404 (1983).
36. J. Klein and B. Eisenmann, *Mater. Res. Bull.* **23,** 587 (1988).
37. B. Eisenmann, H. Jordan, and H. Schäfer, *Z. Naturforsch., B: Anorg. Chem., Org. Chem.* **39,** 1151 (1984).
38. A. Wojakowski, *J. Less-Common Met.* **107,** 155 (1985).